Saruchi *et al.*
Journal of Analytical Science and Technology (2023) 14:12
https://doi.org/10.1186/s40543-023-00374-5

Journal of Analytical Science and Technology

RESEARCH ARTICLE

Open Access

Controlled release of harmful pesticide dichlorvos through synthesized biodegradable aloe vera–acrylic acid-based hydrogel and its utilization in soil water management

Saruchi[1], Vaneet Kumar[2*], Ayman A. Ghfar[3] and Sadanand Pandey[4*]

Abstract

The present work deals with the synthesis of biodegradable hydrogel of a natural polysaccharide aloe vera and vinyl monomer acrylic acid. In this synthesis, ammonium persulfate–glutaraldehyde was used as initiator-cross-linker system, acrylic acid as monomer and aloe vera as backbone. Grafting was confirmed by different techniques like SEM, FT-IR, XRD and EDS. Maximum percentage swelling of synthesized hydrogel was found to be 756%. Biodegradation behavior of synthesized hydrogel [Av-cl-poly(AA)] was studied by soil burial, composting and vermicomposting methods. Maximum biodegradation was found to be 90%, 94% and 93% in case of soil burial, composting and vermicomposting methods, respectively. Biodegradation of Av-cl-poly(AA) was confirmed by FT-IR and SEM techniques. Water retention capacity was prolonged from 11 to 20 days using synthesized Av-cl-poly(AA). Water content of clay soil and sandy loam soil was increased to an extent of 6.1% and 5.79%, respectively. Synthesized Av-cl-poly(AA) has been found to be effective in sustained release of harmful pesticide dichlorvos. The results showed that maximum release of dichlorvos was found to be 1024.34 ppm after 44 h.

Keywords Aloe vera, Acrylic acid, Dichlorvos pesticide, Biodegradation, Water retention

Introduction

Agriculture sector uses a lot of pesticides to control the pest in the field. These pesticides are used in larger quantities than required. Most of these pesticides go into the soil and air and pollute drinking water and environment. These pesticides have disastrous effects on the flora and fauna. Many of these pesticides are carcinogenic and cause many health issues to human beings. So, there is a requirement to control use of these pesticides.

Polymeric materials are designed and chemically transformed to display appropriate properties. They are biocompatible and biodegradable in nature, and they also substantiate the outline of the surface to which they are implemented. They are also called 'smart' or 'intelligent' gels, because they have the property of changing their behavior depending on the outer environment. The cross-linkage makes the grafting insoluble in a solvent owing to electrostatic interaction and the hydrogen bonding strengthens the polymer (Neethu et al. 2018; Abobatta 2019; Mittal et al. 2016).

Properties of the hydrogel to attain large amounts of water, controlled release of agrochemicals and change its

*Correspondence:
Vaneet Kumar
vaneet2106@gmail.com
Sadanand Pandey
sadanand.au@gmail.com; spandey@ynu.ac.kr
[1] Department of Biotechnology, CTIPS, CT Group of Institutions Jalandhar, Jalandhar, Punjab, India
[2] Department of Natural Science, CT University, Ludhiana, Punjab, India
[3] Department of Chemistry, College of Science, King Saud University, P.O. Box 2455, Riyadh 11451, Saudi Arabia
[4] Department of Chemistry, College of Natural Science, Yeungnam University, 280 Daehak-Ro, Gyeongsan, Gyeongbuk 38541, Republic of Korea

behavior with environmental change attained the attention of the researchers to use hydrogel as a solution of agricultural problems, without affecting the environment and fertility of soil. Synthesized polymers were employed to increase the efficacy of the pesticides and herbicides, permitting lesser doses to be used, which ultimately plays an important role to reduce pollution and protects our ecosystem (Saruchi et al. 2019; Ekebafe et al. 2011).

Hydrogels are used in agriculture to increase the porosity of the soil by holding large amounts of water for a prolonged period of time, which reduces the need of irrigation, lower the erosion of soil and thus increase the fertility of soil. Hydrogel helps in controlled release of agrochemicals, which is very necessary for achieving their impactive usage and also reduces the pollution (Motshabi et al. 2022; Naushad and ALOthman 2015; Naushad et al. 2016). Encapsulated natural liquid pesticide neem seed oil, utilizing sodium alginate and glutaraldehyde and the swelling studies revealed insignificant disparity in swelling by stocking variable quantities of neem seed oil (Naushad et al. 2015; Kulkarnia et al. 2000).

The compatibility of silver coated hydrogels was verified, and this system was also used to functionalize polyacrylate hydrogel. The synthesized hydrogels possessed an outstanding water retention ability which was quite beneficial in rain fed agriculture (Saruchi et al. 2016; Faisal et al. 2020). Hydrogel synthesized from acrylic acid, urea, *N*,*N*′-Methylene bis acrylamide (MBA) and ammonium persulfate (APS) at 70 °C in the presence of N_2 atmosphere. During synthesis, the reaction mixture was neutralized with NaOH, due to which the electrostatic repulsions occurring between carboxylate ions increased, and this leads to the expansion of the structure, thereby increasing the water absorption capacity. A super-absorbing hydrogel was synthesized using polyacrylic acid with help of a polymerization method. Acetone and sodium bicarbonate were taken as porogens. MBA and 1, 4-butanediol diacrylate were taken as cross-linking agents (Disha et al. 2016; Mittal et al. 2018, 2020; Saruchi et al. 2013).

Dichlorvos is predominantly used as a pesticide. It is an organophosphate type and long-term exposure of this pesticide causes lots of health issues such as genotoxic, neurological, renal, respiratory, immunological, hepatic, dermal, systemic effects and even leads to death. This is carcinogenic. The reason for its toxicity is due to its capability to hinder acetylcholinesterase at the cholinergic junction of the nervous system (Saruchi et al. 2014, 2015; Cheng et al. 2018).

The botanical name of aloe vera is *Aloe barbadensis*. It is a perennial succulent plant belonging to the liliaceae family. It is also named as a healing plant or a silent healer. It is grown not only for agricultural purposes but also for medicinal use. The main components present in it are amino acid, enzyme, lecithin, lipid, minerals, lactates, salicylate, vitamins, etc. There are 20 types of amino acids present in aloe vera. Aloe vera-based hydrogels are mostly used in biomedical sector and in the dye removal, but no work is dedicated to used such type of hydrogel in controlled release of pesticide. The present work deals with the grafting of natural polysaccharide aloe vera with acrylic acid and monomer using ammonium persulfate as an initiator and glutaraldehyde as cross-linker. Effect of different salt concentration on swelling capacity of synthesized hydrogel was studied. Utilization of synthesized hydrogel for water retention and water-holding capacity was studied. Synthesized hydrogel was used as a device for the controlled release of pesticide dichlorvos. Biodegradability of synthesized hydrogel and impact of biodegraded hydrogel on soil fertility was also investigated.

Experimental

Material

Aloe vera powder (Kshipra Biotech Pvt., Ltd.), acrylic acid, glutaraldehyde (Lobachemie laboratory reagent and fine chemicals), ammonium persulfate (Avantor Performance Material, India Ltd.).

Characterization

Fourier-transform infrared (FT-IR) spectroscopy

This characterization method was utilized in order to get an infrared spectra of the polymer. Fourier-transform spectroscopy collects a very high resolution data for a wide spectrum range. The molecular entity as well as different structures present gets identified by the bands of IR. FT-IR of the polymers under study was procured on PerkinElmer RXI spectrophotometer using KBr pellets (Sigma-Aldrich).

Scanning electron microscopy (SEM)

SEM of the polymers was performed on JSM-6100. The surface morphology of candidate polymer and deviations of candidate polymer on graft copolymerization were studied through scanning electron microscopy (SEM).

X-ray diffraction (XRD) studies

XRD of samples was done on X' Pert Pro. Small particle sizes of each sample were thinly pulverized into powder prior to exposing it to X-ray diffractometry. The X-ray diffraction (XRD) measurements were done with Rigaku Ultima IV diffractometer operating at 40 kV and a current of 30 mA at a scan rate of 0.388 min^{-1} using parallel beam geometry and Cu-Kα radiation. Coherence length of polymers was calculated using the following equation:

$$L = \frac{0.9\lambda}{\beta^{1/2}} \times \cos\phi$$

Here, L = coherence length, λ = wavelength, β½ = full width half maximum and θ = diffraction angle (Kwon et al. 2021; Saruchi and Kumar 2019).

Energy-dispersive X-ray spectroscopy (EDS)

EDS is an analytical technique which is used for the analysis of an element and estimation of its relative abundance. It works on the release of X-rays due to jumping of electron from L to K shell during interaction of high-energy electron and the sample. EDS of the aloe vera and Av-cl-poly(AA) was scrutinized by SU8010, Hitachi (Saruchi et al. 2013).

Preparation of (Av-cl-poly (AA)

Aloe vera (1 g) was added in a reaction flask having 15 mL of distilled water. Then, APS (0.19 mol/L) was added to it followed by addition of glutaraldehyde (0.02 mol/L) with continuous stirring. This was followed by the addition of acrylic acid (3.4 mol/L) to the reaction mixture and was stirred meticulously until homogenous mixture was obtained. Synthesized hydrogel was then dried in hot air oven (50 °C) until constant weight was attained.

Different reaction parameters like concentration of initiator, monomer, cross-linker, reaction time, amount of solvent, temperature and pH were optimized with respect to percentage swelling (Ps) as per equation given below (Mittal et al. 2016; Saruchi et al. 2014, 2019):

$$P_s = \frac{W_s - W_d}{W_d} \times 100$$

where W_s and W_d are weights of swelled and dry Av-cl-poly(AA), respectively (Naushad et al. 2019; Montesanoa et al. 2015; Han et al. 2004).

Swelling studies in various chloride salt solutions

Impact of ionic strength of different positively charged ions of diverse ionic strength like 0.01, 0.02, 0.03, 0.04 and 0.05 mol L^{-1} on Ps of formulated polymers was premeditated in NaCl, KCl, $CoCl_2$. $6H_2O$, $BaCl_2$ and $FeCl_3$ salt solution, at a preoptimized time, temperature and pH (Mittal et al. 2016; Saruchi et al. 2014, 2019).

Biodegradation studies of Av-cl-poly(AA) by soil burial, composting and vermicomposting method

Biodegradation behavior of synthesized Av-cl-poly(AA) was studied by soil burial, composting and vermicomposting methods. The soil utilized for biodegradation studies was taken from the garden of CT Institute, Jalandhar, in case of soil burial method. The compost for the biodegradation study was taken from the waste water release from CT campus, Jalandhar, and vermicompost was purchased from nursery, respectively. The water level was maintained to avoid drying of the soil by evaporation. The compost rich in microbial species was regularly fed to the samples contained in the pot to enrich and nourish the medium with a lot of microbes. Synthesized hydrogel was placed at a distance of 3 cm apart from each other, while placing them in the respective soil sample. Samples were weighed after a regular interval of 7 days. Biodegradation of the samples was confirmed by FT-IR and SEM characterization (Saruchi et al. 2015).

Dichlorvos release from Av-cl-poly (AA)

Loading of dichlorvos in the Av-cl-poly (AA)

2000 ppm aqueous solution of dichlorvos was prepared, and its wavelength for maximum absorption was noted down using a UV–Vis spectrophotometer. The standard curve of the dichlorvos at different concentrations was prepared at the noted wavelength. Av-cl-poly (AA) was immersed in the prepared dichlorvos solutions for 24 h. After 24 h, the dichlorvos-loaded hydrogel was taken out of the solution, wiped out and dried in a hot air oven. After drying, it was washed with distilled water so as to remove any surface adhered dichlorvos particles. Then, dichlorvos release was studied at neutral pH and at ambient temperature after every 4 h interval. The concentration of agrochemical release was studied using a double beam UV–VIS spectrophotometer (Saruchi et al. 2016, 2019).

Mathematical analysis of dichlorvos release behavior

Dichlorvos release behavior of Av-cl-poly(AA) was studied with a mathematical model. The generalized empirical equation has been used to describe the dichlorvos release behavior from the Av-cl-poly(AA). The empirical equation used to describe the liquid uptake, i.e., weight gain (M_s), can be calculated as:

$$M_s = Kt^n$$

where 'K' and 'n' are constants. 'n' = 0.5 reveals the Fickian diffusion, and the value of 'n' = 1.0 signifies Case II diffusion. Non-Fickian or anomalous diffusion occurs if the value of 'n' lies between 0.5 and 1.0. Dichlorvos release from the Av-cl-poly(AA) can be evaluated from the power law equation, where M_s is replaced with M_t/M_∞ and the modified expression is as under:

$$\frac{M_t}{M_\infty} = Kt^n$$

where M_t is the fractional release of drug and agrochemical at different time intervals, M_∞ is the release of dichlorvos at equilibrium, and 'K' is the constant of the matrix.

'*n*' is the diffusion exponent of the dichlorvos release mechanism. The equation can be applied for the 60% release of the total drug and agrochemical. The slope and intercept of the plot between M_t/M_∞ versus ln*t* gives the value of '*n*' and '*K*' (Kaith et al. 2012).

Diffusion coefficient of dichlorvos release

Diffusion process can be described by Fick's first and second law. Initial, average and lateral diffusion coefficients were calculated from the equation:

$$\frac{M_t}{M_\infty} = 4x\frac{D_I}{\pi l^2}$$

Here, D_I is the initial diffusion coefficient, M_t/M_∞ is the fractional release, and M_t and M_∞ are the dichlorvos release at time '*t*' and at equilibrium, respectively. *l* is the thickness of the sample.

Average diffusion coefficient can be calculated from the equation given below:

$$D_A = \frac{0.049l^2}{t^{1/2}}$$

where $t^{1/2}$ is the time required for the 50% release of drugs.

Lateral diffusion coefficient can be calculated from the equation given below:

$$\frac{M_t}{M_\infty} = 1 - \left(\frac{8}{\pi^2}\right)\exp\left(-\frac{\pi^2 Dt}{l^2}\right)$$

The slope of the plot between $\ln(1 - M_t/M_\infty)$ and time t has been used for the evaluation of D_L.

$$D_L = \left(\text{slope}\frac{l^2}{8}\right)$$

Measurement of water retention capacity of soil by Av-cl-poly(AA)

Water retention capacity of soil using Av-cl-poly(AA) was studied in two types of soils: clay soil and sandy loam soil. Five samples 0.5 g, 1.0 g, 1.5 g, 2.0 g and 2.5 g of each synthesized hydrogel Av-cl-poly(AA) were mixed thoroughly with 50 g of dry soil in a disposable container separately. Then, 100 mL of water was added and the initial weight of the sample was taken. Containers having soil and water, without hydrogel, were referred as control, while the containers with hydrogels were taken as test samples. Regularly up to 25 days weights of the samples were taken and water retention capabilities of the soil with and without hydrogel were studied. Residual water (g/g) was calculated from the equation given below (Saruchi et al. 2019):

$$\text{Residual water} = \frac{W_f - W_i}{W_i}$$

where W_f and W_i are the final and initial weights of the samples, respectively.

Measurement of water uptake by clay and sandy loam soils using swollen hydrogel

Two different soil samples clay and sandy loam were taken for this experiment. Soil samples were collected from the upper layer (0–50 cm). Then, soils were air-dried. Known amounts of dried Av-cl-poly(AA) were kept in tea bags and immersed in 100 mL of water, so as to soak water for 24 h. After 24 h tea bags were taken out from the water and gently wiped with tissue paper, so that excess water can be removed. Then, these tea bags were kept in dry clay and sandy loam soils. After interval of 4 h, these tea bags were weighed until the equilibrium was attained (Saruchi et al. 2013; Saruchi and Kumar 2019).

Results

Characterization

Fourier-transform infrared (FT-IR) spectroscopic studies

FT-IR of the synthesized polymers was performed on the PerkinElmer spectrophotometer. IR spectrum of aloe vera showed wider peak at 3325 cm^{-1} because of O–H stretching of OH group, 2915 cm^{-1} because of C–H stretching of C–H group, 2101 cm^{-1} due to C≡C elongation of mono-substituted group, 1607 cm^{-1} because of carbonyl group of COOH, 1345 cm^{-1} because of C–O stretching of tertiary alcohol, 1237 cm^{-1} because of C–C deformation in the methyl group (Fig. 1a). On the other hand, IR spectrum of Av-cl-poly(AA) showed supplementary tips at 2931 cm^{-1} of C–H stretching, 2659 cm^{-1} O–H of carboxylic acid, 1699 cm^{-1} of C=O stretching of aryl carboxylic acid, 1416 cm^{-1} C–H stretching because of C–H group, 1160 cm^{-1} because of C–C stretching of C–C group (Fig. 1b).

Scanning electron microscopic (SEM)

The surface morphology of the synthesized candidate polymer on grafting was studied through SEM. Scanning was synchronized with the microscopic rays upholding a small size over a large distance. SEM was performed on JSM-6100. The surface morphology of the aloe vera and Av-cl-poly(AA) was studied by the SEM technique. SEM images of both the samples exhibited morphological differences. Smooth surface was observed in SEM of backbone, aloe vera (Fig. 2a). The surface morphology of backbone did not exhibit any kind of ridges, grooves or pits as observed in figure. Rough surface-bearing depressions and pits were observed extending throughout the

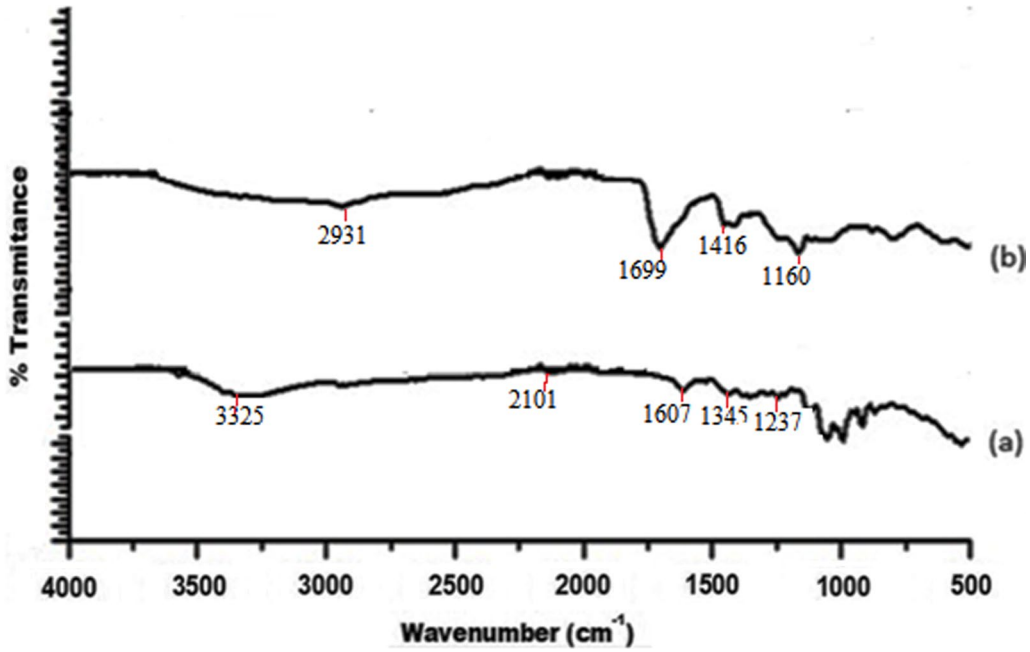

Fig. 1 **a, b** FT-IR spectra of **a** aloe vera and **b** Av-cl-poly(AA)

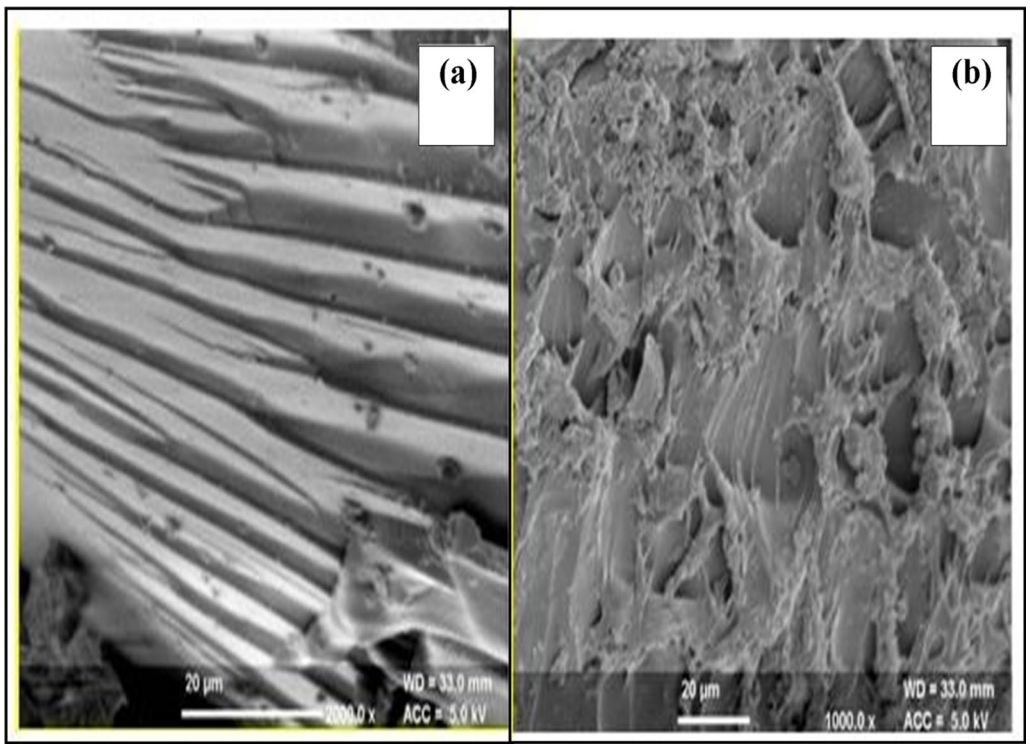

Fig. 2 **a, b** SEMs of **a** Aloe vera and **b** Av-cl-poly(AA)

surface of Av-cl-poly(AA), which is not seen in backbone (Fig. 2b). The occurrence of such coarse and porous structures in Av-cl-poly (AA) proves the morphological difference by chemical modification of the backbone through grafting as well as cross-linking brought about by covalent bonding in-between polymeric chains on cross-linking through MBA.

X-ray diffraction (XRD)

XRD of aloe vera and Av-cl-poly(AA) has been explored by X' Pert Pro and showed the disparity in the anisotropy of aloe vera and Av-cl-poly(AA).

The coherence length of the samples was calculated by Scherrer equation. The coherence length of aloe vera was found to be 0.542 Å.

$$L = 0.9\lambda/\beta^{1/2} \times \cos\theta$$

where L = coherence length, λ = wavelength, θ = diffraction angle, and $\beta^{1/2}$ = full width half maximum. XRD of backbone is shown in Fig. 3a. In Av-cl-poly(AA), the rationality (coherence) length is found to be 0.8092 Å, which is higher than the backbone, which showed that the backbone becomes more crystalline by grafting and cross-linking it with acrylic acid. This is because of the influence of increased cross-linker concentration, thereby enhancing the cross-linking density in-between polymeric chains and hence resulting in greater aligned crystalline lattices. Anisotropy increased with increase in coherence length. It proves that acrylic acid has been grafted on backbone demonstrating successful grafting. XRD of Av-cl-poly (AA) is shown in Fig. 3b.

Energy-dispersive X-ray spectroscopy (EDS):

EDS is used for analytical examination of the present elements as well as for the estimation of its relative abundance. It includes an interactive communicative interaction in-between X-ray source as well as sample. A high-energy beam of electrons is focused onto the sample under study. The incident beam causes the excitation of electrons, ejecting them and creating a hole. The electron from higher energy level shifts to the hole, and consequently, difference in energy of higher and lower energy shells gets escaped in the form of X-ray. Carbon, oxygen and nitrogen were found to be the main elements present in aloe vera backbone. It was found that the atomic % of carbon in the backbone was 53.02%. The atomic percentages of oxygen and nitrogen in backbone were determined to be 42.77% and 4.22%, correspondingly (Fig. 4a). Carbon, oxygen and nitrogen were found to be the main elements present in Av-cl-poly(AA). It was found that the atomic % of carbon was 55.22%. The atomic percentage of oxygen and nitrogen was 42.35% and 2.43% (Fig. 4b). The decrease in atomic % of oxygen is because of the exclusion of H_2O molecule.

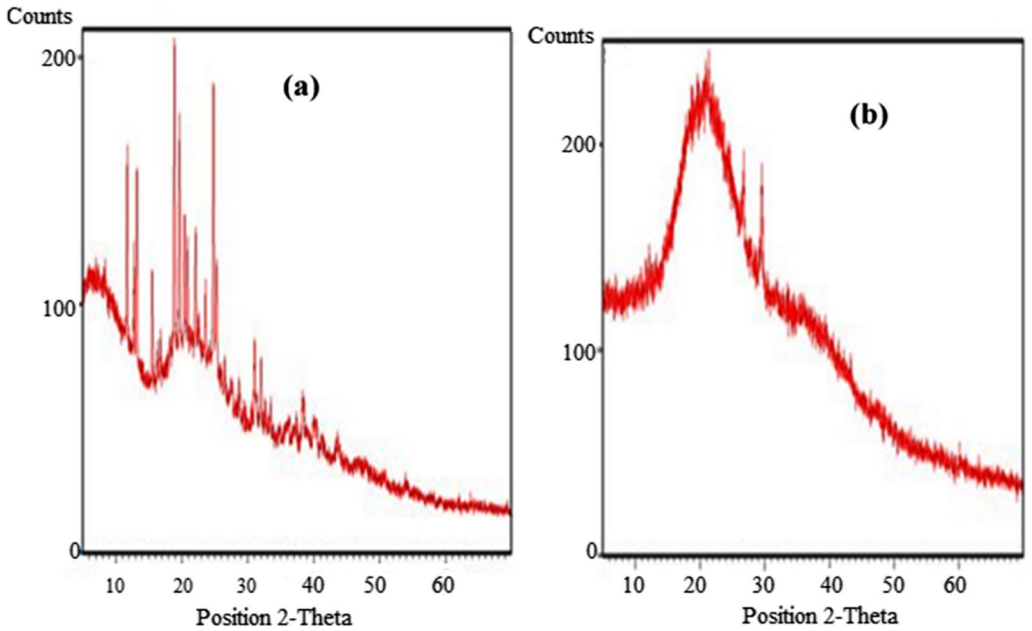

Fig. 3 **a, b** XRDs of **a** aloe vera and **b** Av-cl-poly(AA)

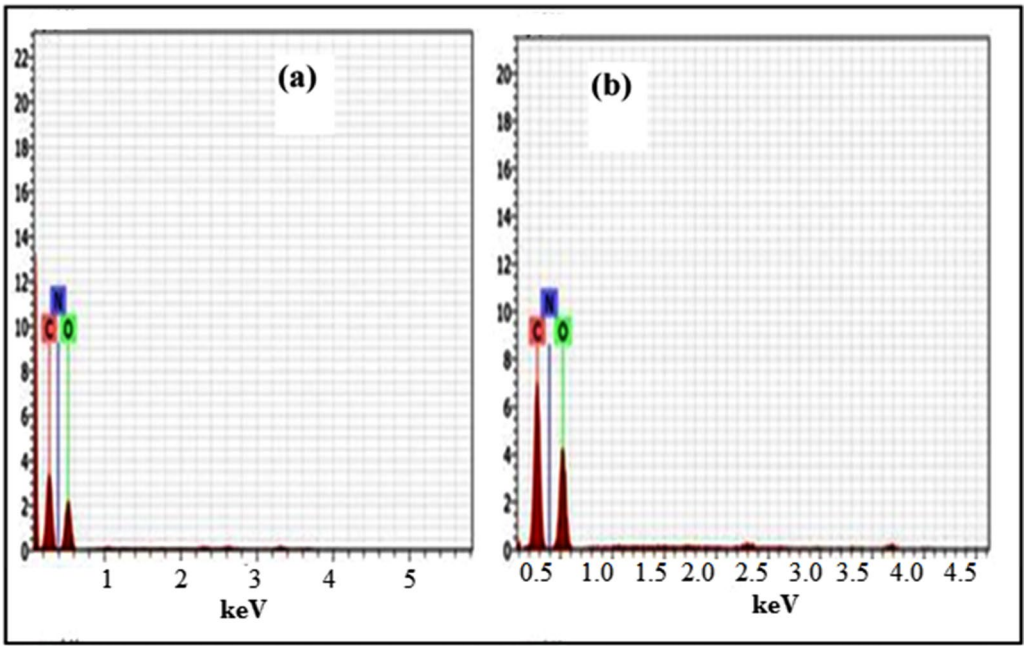

Fig. 4 **a, b:** EDS of **a** aloe vera and **b** Av-cl-poly(AA)

Discussion

Optimization of reaction parameters of Av-cl-poly(AA)

Impact of reaction time

It is clear from Fig. 5a that Ps rises with upsurge in reaction time and achieving 629 % of swelling at a time interval of 75 min. However, further increase in reaction time resulted in decrease in Ps. Percentage swelling primarily increases with time, and it may be pertaining to enhance the interactions between *OH and substrate that leads to activation of active sites on backbone as well as monomer chains, ensuing in improved Ps. Further increment in reaction time will cut down the Ps. It may be due to the preponderance of homo-polymerization over graft copolymerization. Homo-polymerization boosts the viscosity of the reaction medium, by this means putting impediments in the path of free radicals approaching active sites. Therefore, Ps decreases (Guilherme et al. 2015; Nagarjuna et al. 2016).

Impact of reaction temperature

Maximum Ps (569 %) was obtained at 50 °C, but further rise in temperature decrease in Ps (Fig. 5b). This may be due to the reason that, upsurge in the temperature above the optimal point, kinetic energy of free radicals rises, inferring in enhanced conflicts as well as termination reactions. Abstraction of hydrogen ions and homo-polymerization at high temperature lead to decrease in Ps. Furthermore, with rise in temperature, the elasticity of polymer matrix upshots and some additional hydrogen bonds are formed. But beyond optimum temperature, the hydrogen bonds break down, thereby lowering the Ps (Hussein et al. 2017).

Impact of pH

Maximum Ps (502%) was scrutinized under neutral medium (Fig. 5c). Ps was observed to diminish in acidic and basic medium that might be because of premature cessation of polymerization reaction. It might also be owing to repression in the formation of persulfate ions.

Impact of initiator ratio

It is noted that percent swelling increases with increase in the amount of APS and reaches an optimum value 756% (Fig. 5d). Initially, $SO4^{-*}$ and *OH ion concentration increased resulting in generation of more active sites, thereby increasing Ps. But increase in APS concentration beyond the optimum level decreases the Ps due to release of large amounts of hydroxyl and sulfate ions in the reaction mixture, which leads to the termination of the reaction (Kowalski et al. 2019).

Impact of amount of solvent

Increase in the amount of solvent resulted in increased Ps, and at a certain optimum point the Ps starts decreasing. Maximum Ps of 732% was obtained using 15 mL of solvent during grafting (Fig. 5e). It could be

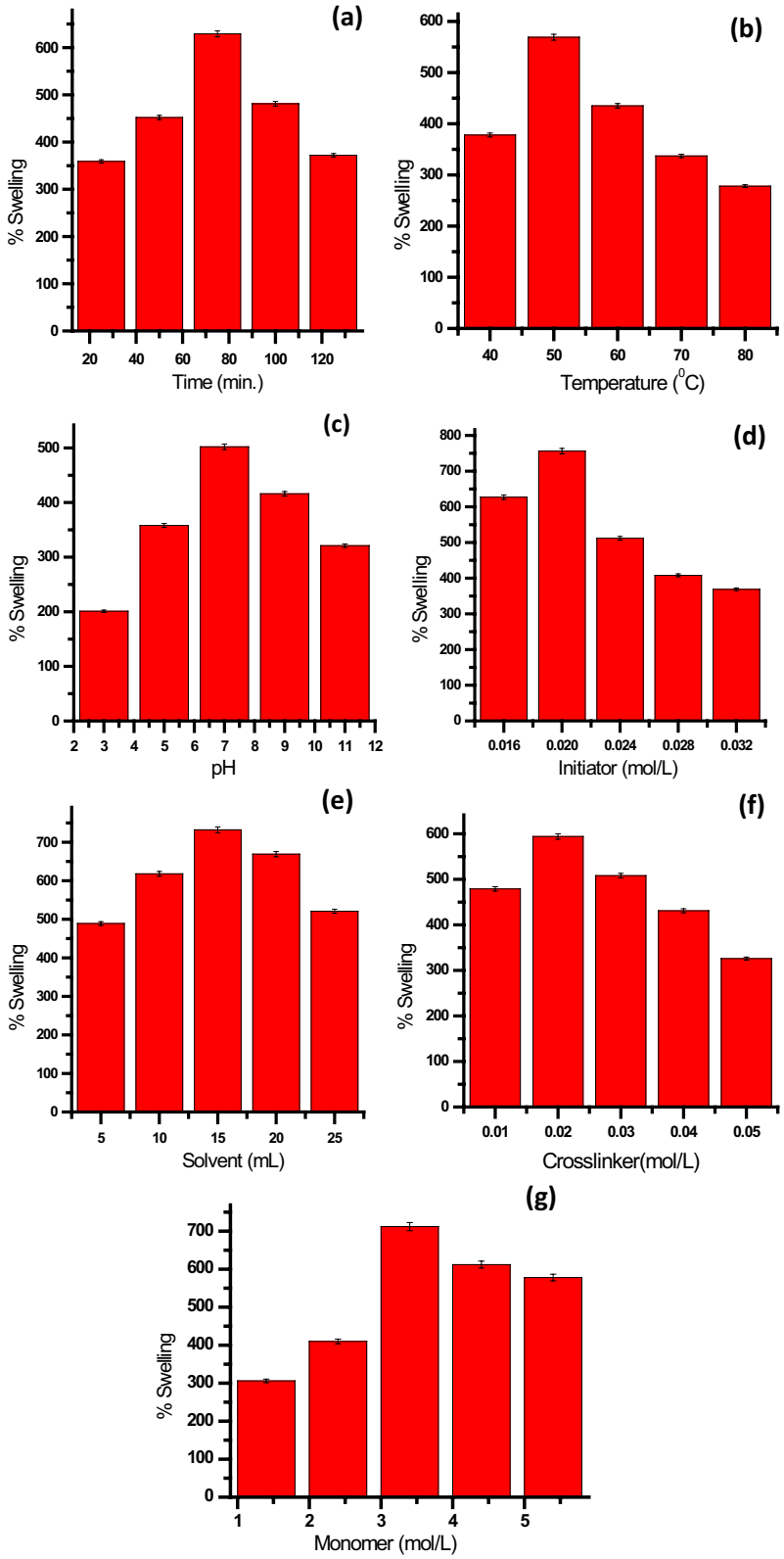

Fig. 5 **a–g** Impact of **a** time; **b** temperature; **c** pH; **d** initiator concentration; **e** solvent; **f** cross-linker concentration; and **g** monomer concentration on Ps of Av-cl-poly (AA)

explained on the ground that initially there was ample amount of *OH concentration, which propagated the polymerization reaction up to some optimal level. However, any further increase in solvent leads to the end of polymerization reaction because of generation of excessive *OH concentration (Saruchi et al. 2013, 2016).

Impact of cross-linker concentration

The optimum amount of glutaraldehyde for the reactions was 0.02 $molL^{-1}$ (594%) (Fig. 5g). An increase in cross-linker concentration above optimum concentration leads to decrease in Ps. Initially, Ps increases because the surface area of the grafted cross-linked moiety increases. But further increase in the concentration of cross-linker leads to compacting of polymeric chains. Thereby, decreasing pore size further leads to desorption and thus reduced the percentage swelling (Saruchi et al. 2013).

Impact of monomer concentration

Maximum Ps, 712%, was observed at acrylic acid concentration of 3.4 mol L^{-1}. Increasing acrylic acid concentration above optimum concentration decreases Ps (Fig. 5f). It may be due to the fact that further increase in the amount of monomer predominates the homopolymerization over grafting. Moreover, the cross-linking density increases and Av-cl-poly(AA) becomes more compact. Moreover, the accessibility of water molecules toward functional groups present in the polymeric chain also decreases, thereby decreasing the Ps (Saruchi et al. 2013; Hussein et al. 2017).

Swelling studies of Av-cl-poly (AA) in deionized water

Swelling behavior of Av-cl-poly(AA) was studied as a function of time, temperature and pH of the swelling medium.

Impact of time on percent swelling

Av-cl-poly(AA) showed utmost swelling of 242% at 2160 min, and thereafter, Ps decreases with further increase in time (Fig. 6a), because the porous network was already saturated and did not accommodate any more solvent molecules with further increase in time (Kumar et al. 2015; Thakur et al. 2018).

Impact of temperature on percent swelling

Impact of temperature on swelling behavior of Av-cl-poly(AA) was studied at different temperatures (40, 50, 60 and 70, 80 °C) at preoptimized time (Fig. 6b). It was found that Ps increased with the increase in temperature and maximum Ps was achieved at 70 °C (Ps = 552%). Further increase in temperature beyond optimized temperature leads to decrease in Ps. This may be due to the fact that with increase in the temperature, the flexibility of the Av-cl-poly(AA) matrix also increases, as a result of which the disruption of secondary interactions takes place, thereby generating more spaces for diffusion of water molecules. Above optimum temperature, the matrix obtained started to collapse, which led to desorption and consequently decreasing swelling (Thakur et al. 2018).

Impact of pH on Ps of Av-cl-poly (AA)

Maximum Ps (556 %) of Av-cl-poly(AA) was recorded in the neutral medium (Fig. 6c). This can be explained on the basis that in the neutral medium, there are a sufficient number of hydrogen ions and it protonates the functional group present in the polymer, as a result of which the polymeric chains are repelled, allowing more water molecules into the matrix, thereby increasing the percentage swelling. In an alkaline medium, the de-protonation of the functional groups takes place, due to which repulsions in-between the polymeric chains decreases. The rigidity of the structure increases, thereby reducing Ps (Kumar et al. 2015; Thakur et al. 2018).

Impact of ionic strength and ionic charge on Ps of Av-cl-poly(AA)

Ionic strength of different cations (Na^{+}, K^{+}, $Ba^{2+,}$ $Co^{2+,}$ Fe^{+3}) on the Ps of Av-cl-poly(AA) in different chloride salt solutions was examined (Fig. 6d). It was noted that with increase in ionic strength of cation, there is a sharp decline in Ps in respective salt solutions. Decrease in Ps with increase in ionic strength of cations might be due to the reverse osmosis process. It was also found that increase in ionic strength of cations leads to increase in the concentration of mobile ions in solution, which leads to decrease in the osmotic swelling pressure (π ions), thus leading to decrease in Ps. It was found that increase in cationic charge led to decrease in Ps, and this may be due to the fact that increase in ionic charge leads to increase in proportionate of cationic–cationic repulsion, which do not permit further access of solution containing cations in the cross-linked network by this means ensuing in desorption of cations. Maximum Ps 248%, 268%, 250%, 236% and 182% was found in NaCl, KCl, $BaCl_2$, CoCl. 6 H_2O and $FeCl_3$ salt solutions having 0.01 $molL^{-1}$ ionic strength of Na^{+}, K^{+}, Ba^{+2}, Co^{+2} and Fe^{+3}, correspondingly (Kumar et al. 2015; Thakur et al. 2018).

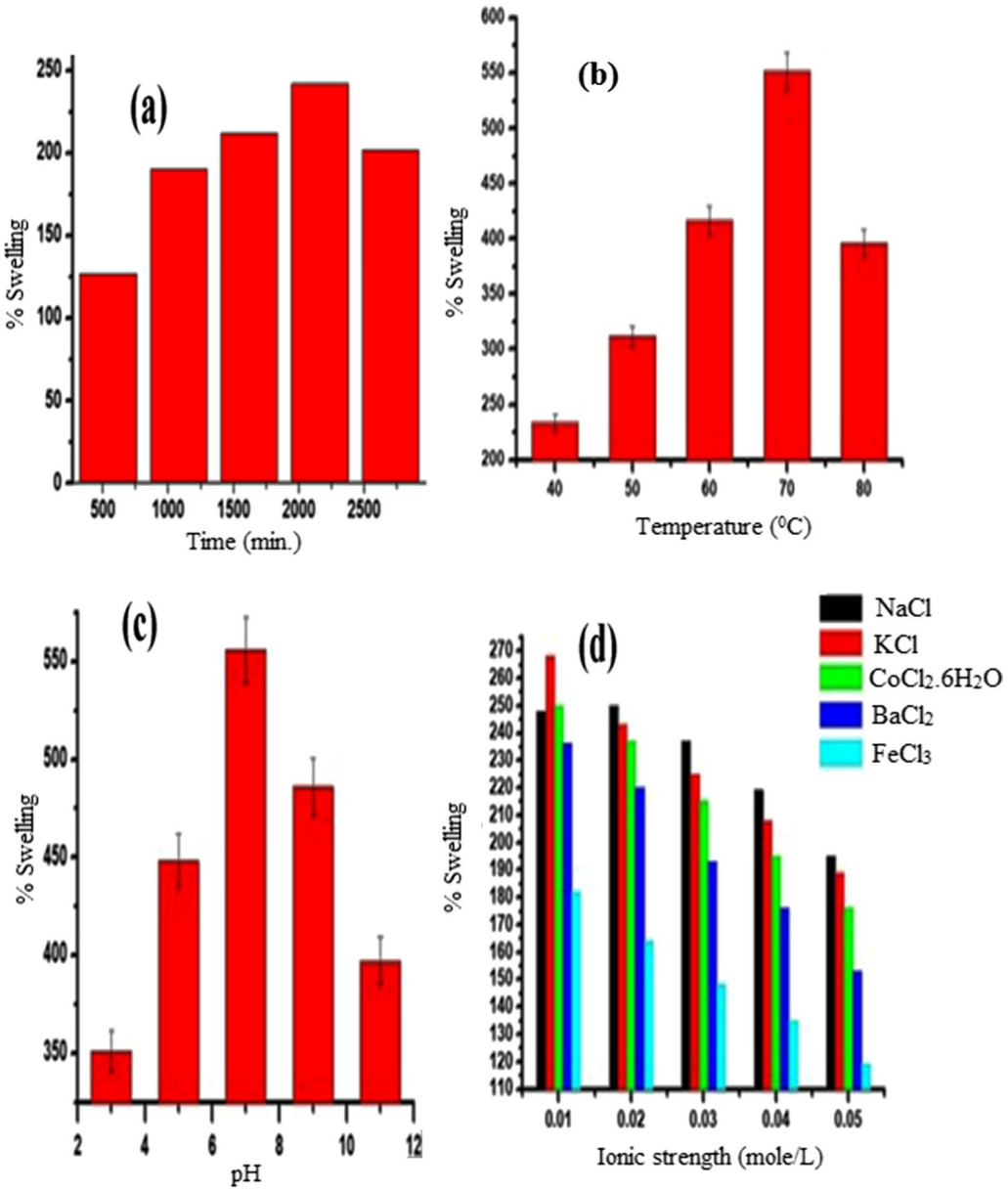

Fig. 6 **a–d** Impact of **a** time; **b** temperature; **c** pH; and **d** ionic strength on Ps of Av-cl-poly (AA)

Table 1 Biodegradation study of synthesized Av-cl-poly(AA) through soil burial, composting and vermicomposting method

Percentage weight loss at different time intervals (Days)										
Biodegradation method of Av-cl-poly(AA)	7	14	21	28	35	42	49	56	63	70
Soil Burial method	7	14	22	30	39	47	59	70	81	90
Composting method	9	16	24	32	42	50	61	72	83	94
Vermicomposting method	8	16	23	30	40	49	60	70	81	93

Biodegradation study of synthesized Av-cl-poly(AA)

Biodegradation behavior using soil burial method

Synthesized polymers were subjected to biodegradation, and the process was carried for a time period of 70 days. Maximum weight loss due to biodegradation of Av-cl-poly(AA) was found to be 90%, after 70 days (Table 1). The degradation of Av-cl-poly(AA) occurred because of the disruption of covalent bonds by microorganisms present in the soil, disintegrating bulky molecular species into simpler ones (Mahinroosta et al. 2018; Michalik and Wandzik 2020).

Biodegradation using composting method

It was observed that Av-cl-poly(AA) underwent degradation in 70 days in compost soil. Maximum weight loss due to biodegradation through the composting method was found to be 94% after 70 days (Table 1). Biodegrading of the Av-cl-poly(AA) occurred by enzymatic and chemical decomposition. The microbe-rich composting material leads to the enzymatic and chemical decomposition, which cleaves the chemical bond of Av-cl-poly(AA), and hence, disintegration takes place. Compost provides nitrogen to bacteria and fungi, which are helpful in degrading polymeric structure. Diverse phases of biodegradation were verified through FT-IR and SEM.

Biodegradation using vermicomposting method

It was observed that synthesized hydrogel underwent maximum degradation 93% with vermicomposting method in 70 days (Table 1). The microorganism causes chemical and enzymatic decomposition of the Av-cl-poly(AA), thereby cleaving the chemical bond, and leads to disintegration of Av-cl-poly(AA). Biodegradation was further verified via FT-IR and SEM.

Evidences of biodegradation through FT-IR

A great distinction in peak positions of FT-IR of biodegraded hydrogel is observed because hydrolysis and enzymatic reactions occurred at the time of biodegradation. At the initial stage biodegradation was slow, but with the passage of time it was increased, this can be explained on the basis in the initial stage surface of the synthesized hydrogel was hard and it took time for the microorganism to invade in it, but as the time increased the hydrogel was exposed to moisture and it became soft and easily accessible to the microorganism (Mittal et al. 2018). It was found that the peaks, which were seen in Av-cl-poly(AA) before biodegradation (Fig. 1a) on 2128–1864 cm^{-1}, were missing during first stage of biodegradation and some of the peaks 2931–2659 cm^{-1} and 1699–1051 cm^{-1} were shifted as shown in Fig. 7a, d, g. In the second biodegradation phase, peaks observed at 3427 cm^{-1} and 1453 cm^{-1}in the first stage were found missing and some of the peaks at 3088–1921 cm^{-1} were shifted (Fig. 7b, e, h). This may be due to the degeneration of cross-linking between aloe vera and poly acrylic acid chains. In the third stage of biodegradation, peaks observed at 3870–3388 cm^{-1}, 3068–2898 cm^{-1} and peak at 2321 cm^{-1}were missing and peaks corresponding to 3152 cm^{-1}, 2656–2575 cm^{-1} and 2114–1404 cm^{-1} were shifted as shown in Fig. 7c, f, i, and this may be due to the fact that intensity of peak due to –OH group present over backbone was found to decrease progressively because of biodegradation. The missing and the shifting of the peaks showed that the synthesized hydrogel is biodegradable as well as eco-friendly in its nature.

SEM studies of various biodegradation stages of Av-cl-poly(AA)

SEM results revealed that the biodegradation of hydrogel occurred at different phases as shown in Fig. 8a–i. The apparent fissures were seen in the first stage of biodegradation. The concentration of morphological smash up enlarged with the rise in biodegradation moment (Fig. 8a, d, g). In the second phase of biodegradation, big crevices with further superficial pits were observed (Fig. 8b, e, h). SEM images clearly showed that in the third stage of biodegradation, complete disintegration of Av-cl-poly(AA) occurred (Fig. 8c, f, i).

Release kinetics of dichlorvos through the polymer matrices

Synthesized Av-cl-poly(AA) has been found to be effective in sustained release of dichlorvos. The results showed that maximum release of dichlorvos occurred after 44 h (Fig. 9a). The maximum release of dichlorvos was found to be 1024.34 ppm ($n = 0.99$, $K = 1.6$) (Fig. 9a–d). The diffusion mechanism was found to be non-Fickian, which means dichlorvos release rate was equivalent to the relaxation time of the hydrogel matrix. The value of initial diffusion coefficient and lateral diffusion coefficient depicted that lateral diffusion coefficient has higher value than initial diffusion coefficient (Table 2). This was due to the fact that in the beginning dichlorvos-loaded matrix swells slowly, this allows the slow diffusion of dichlorvos, which further increases with increase in swelling until equilibrium was attained.

Water retention capacity of soil through Av-cl-poly(AA)

As the population is increasing and agricultural land is decreasing, there is a need to increase agricultural production. This leads to the attention of utilization of hydrogel in agriculture as a novel soil conditioner. Agricultural hydrogel has the capacity to retain water granules

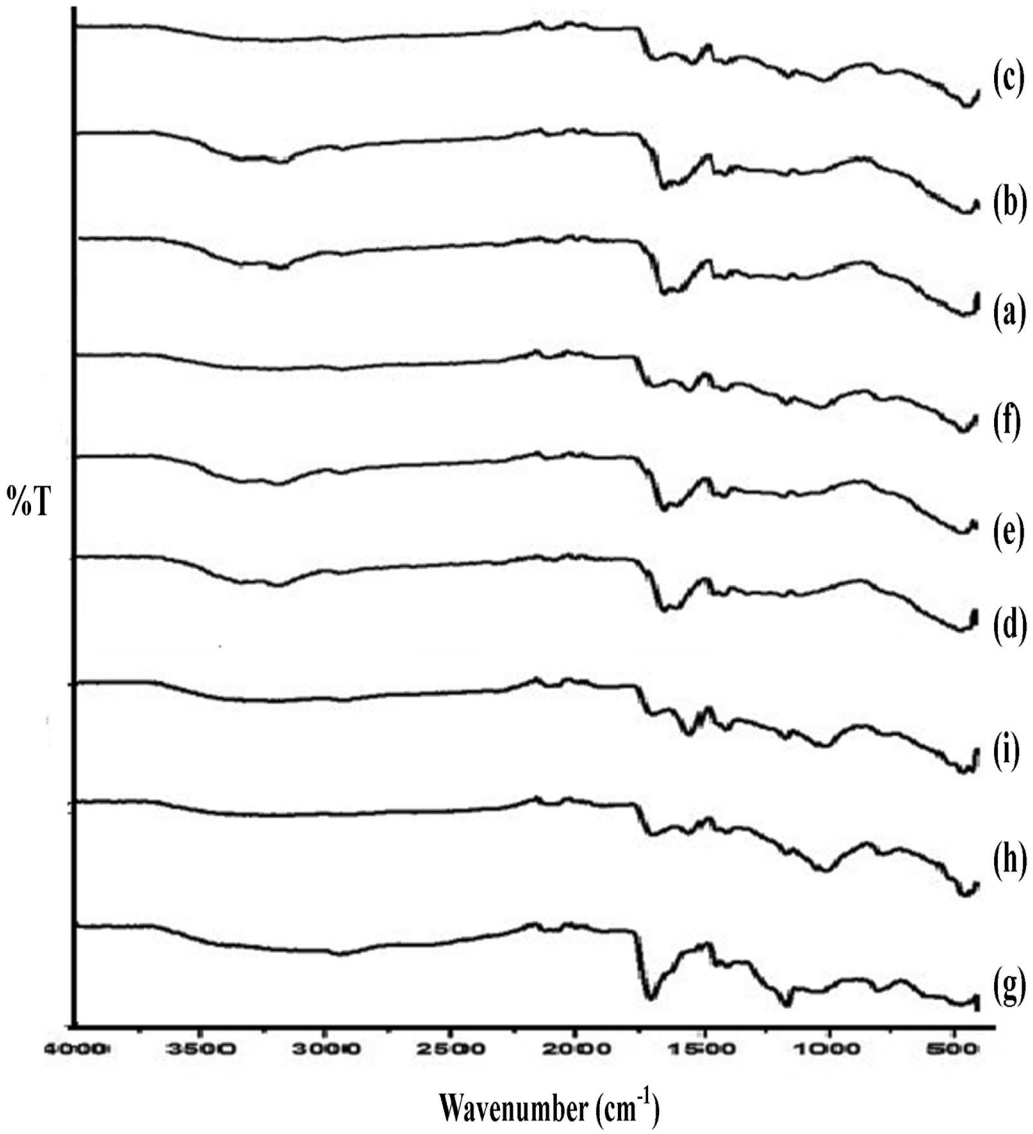

Fig. 7 **a–i** FT-IR spectra of biodegradation of **a** Av-cl-poly(AA) stage-I; **b** Av-cl-poly(AA) stage–II and **c** Av-cl-poly(AA) stage-III using soil burial method **d** Av-cl-poly(AA) stage-I; **e** Av-cl-poly(AA) stage–II and **f** Av-cl-poly(AA) stage-III using composting method; **g** Av-cl-poly(AA) stage-I; **h** Av-cl-poly(AA) stage–II; and **i** Av-cl-poly(AA) stage-III using vermicomposting method

for a longer period of time, as they swell many times to their original size, when they come in contact with water. These characteristics of the hydrogel make them utilized in agriculture and in desert areas. So in the present study hydrogel was used as a water retaining device. Soil mixed with Av-cl-poly(AA) showed lesser water evaporation as compared to the soil without hydrogel. Residual water left in the control sample was 0.08 g/g in clay soil and 0.1 g/g in sandy loam soil after11 days. Whereas, in soil mixed with 2.5 g of Av-cl-poly(AA) water retention capacity prolonged for 20–21 days in clay and sandy loam soil, respectively. The residual water content was found to be 0.56 g/g and 0.63 g/g (Fig. 10a, b) in clay and sandy loam soil, respectively. It was clear from the results that water loss from the soil was decreasing with increase in hydrogel amount (Chen et al. 2018; Ramli 2019; Hidangmayum et al. 2019).

Water uptake by soil samples using swollen Av-cl-poly(AA)

Water content of the clay and sandy loam soil was increased using swollen Av-cl-poly(AA). It was found that the addition of a small amount of swollen Av-cl-poly(AA) (up to 1%) in dry clay and sandy loam soils leads to increase in the water content of the respective soil.

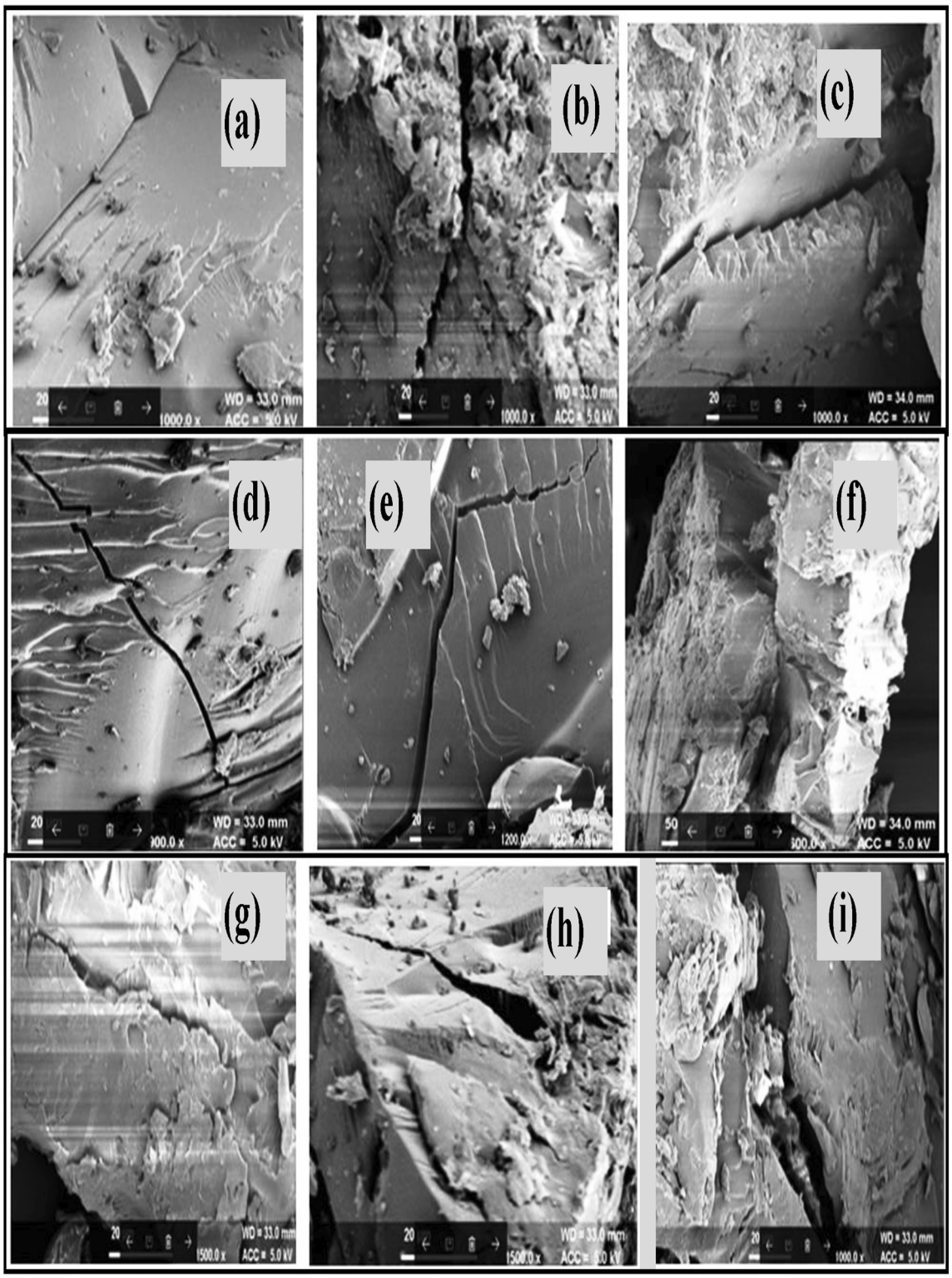

Fig. 8 **a–i** SEMs of biodegradation of **a** Av-cl-poly(AA) stage-I; **b** Av-cl-poly(AA) stage-II and **c** Av-cl-poly(AA) stage-III using soil burial method; **d** Av-cl-poly(AA) stage-I; **e** Av-cl-poly(AA) stage–II and **f** Av-cl-poly(AA) stage-III using composting method; **g** Av-cl-poly(AA) stage-I; **h** Av-cl-poly(AA) stage–II; and **i** Av-cl-poly(AA) stage-III using vermicomposting method

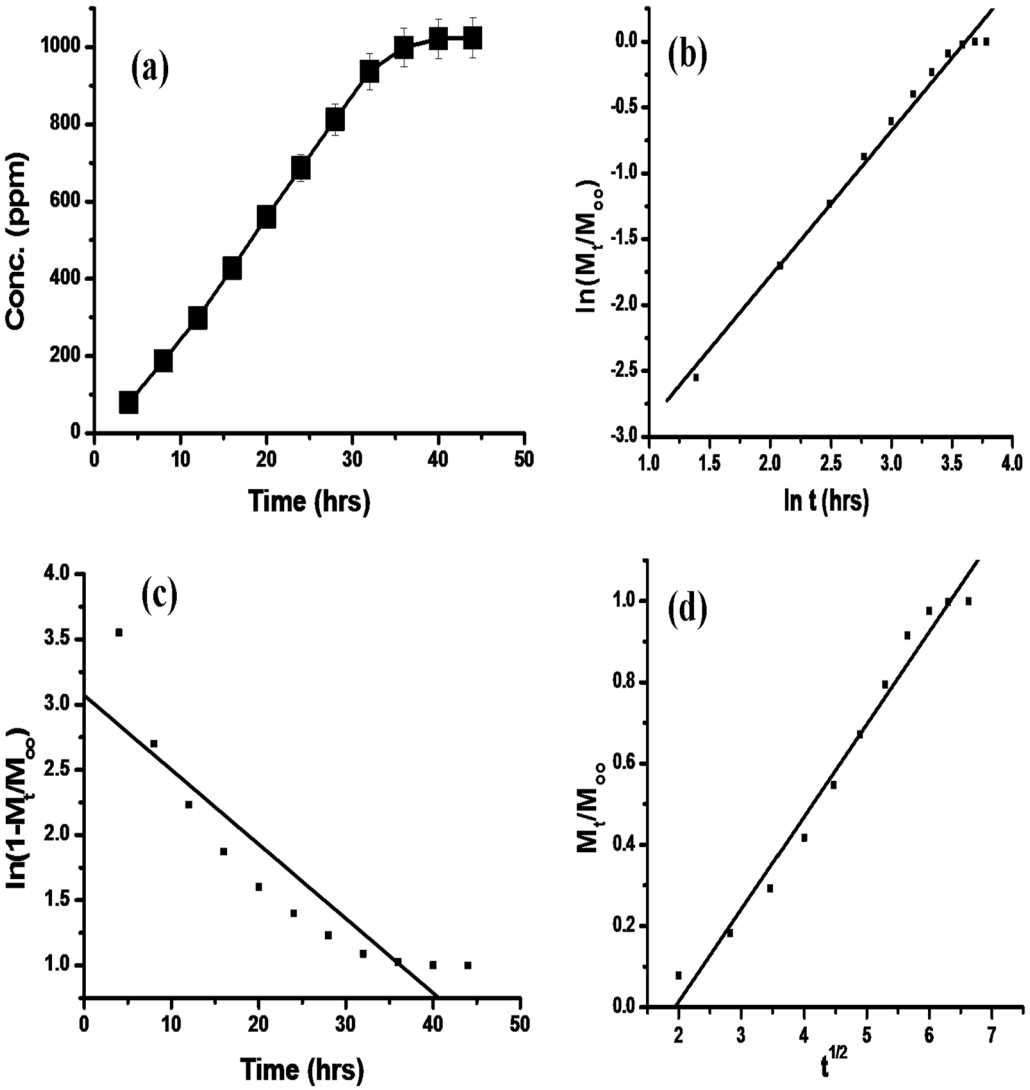

Fig. 9 **a–d** Release behavior of dichlorvos through Av-cl-poly(AA) at different time intervals **a** conc. versus time; **b** ln(M_t/M_∞) versus lnt; **c** ln(1 − M_t/M_∞) versus time and **d** M_t/M_∞ versus $t^{1/2}$

Table 2 Diffusion exponent, gel characteristic constant and diffusion coefficients for the release of dichlorvos through Av-cl-poly(AA)

	Diffusion exponent '*n*'	Gel characteristic constant '*K*'	Diffusion coefficient (m^2/h)		
Av-cl-poly(AA)	0.99	1.68	$D_I \times 10^{-7}$	$D_A \times 10^{-7}$	$D_L \times 10^{-7}$
			1.07		1.32
			0.20		

Water content in the soil was increased until the attainment of equilibrium after 36 h. It is clear from the results that 1.0% addition of Av-cl-poly(AA) to the clay and sandy loam soil increased the water content to the extent of 6.1% and 5.79%, respectively (Fig. 11a, b). There is no further increase in the water uptake with further increase in time, because the equilibrium was attained between the soil sample and Av-cl-poly(AA). It was clear from the results that the synthesized hydrogel is very effective for the water release purpose in different soil, without having any adverse impact on the soil. This showed that synthesizing hydrogel increases the soil texture and porosity of the soil, which ultimately may lead to the enhancement of soil fertility (Hidangmayum et al. 2019).

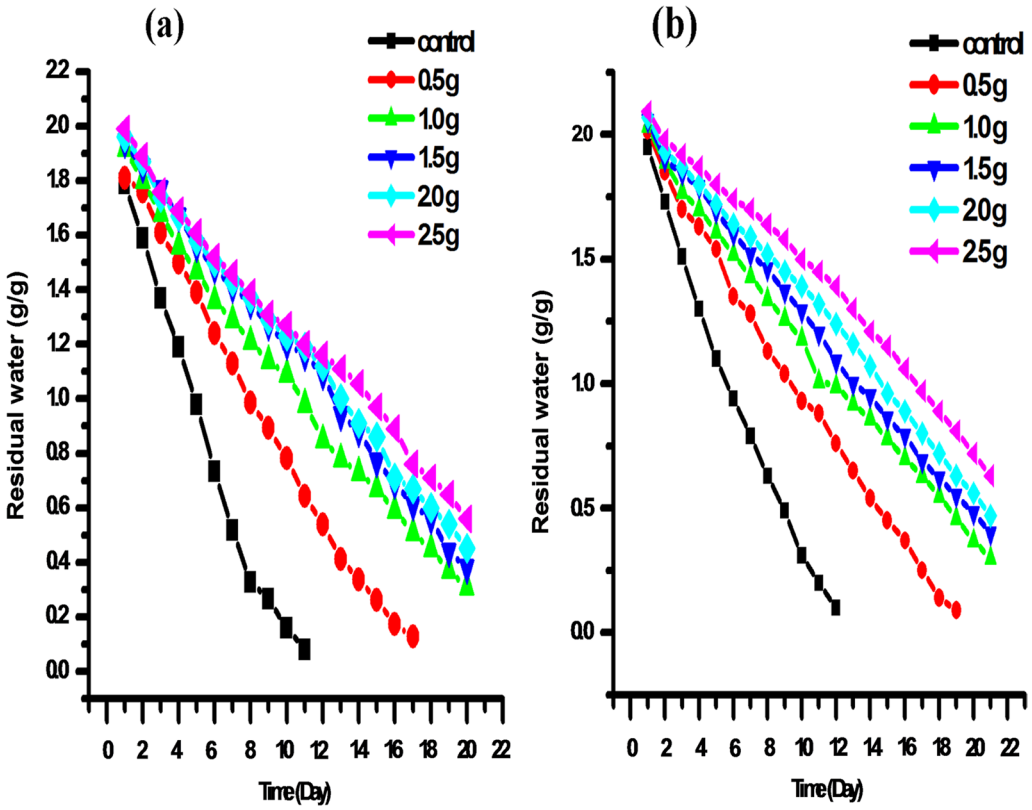

Fig. 10 **a, b** Water retention capacity of **a** clay soil and **b** sandy loam soil using Av-cl-poly(AA)

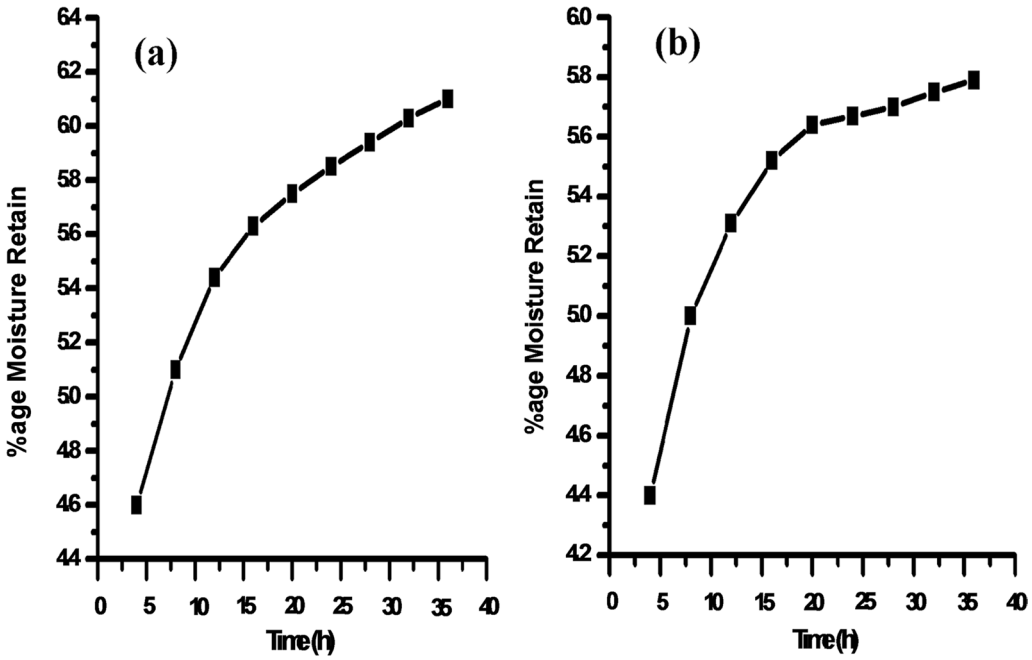

Fig. 11 **a, b** Water retention capacity of **a** clay soil and **b** sandy loam soil using Av-cl-poly(AA)

Table 3 Analysis of soil samples containing biodegraded Av-cl-poly(AA)

S. No.	Samples	pH	Organic carbon (%)	Phosphorus (g/m^2)	Potassium (g/m^2)
1	Control	6.9	0.31	12.5	59
2	Av-cl-poly(AA)	6.7	0.36	13.1	59

Impact of biodegradation of synthesized hydrogel on soil

Biodegraded hydrogel impact on soil fertility was studied by carrying out the soil analysis before and after biodegradation of hydrogel. Organic carbon, phosphorus, potassium contents and pH of the soil sample were analyzed.

The results revealed that pH of the control soil was pH 6.9 and organic carbon was 0.31%. Phosphorus and potassium content was 12.5 g/m^2 and 59 g/m^2, respectively (Table 3).

It is well known that carbon is the one of the constituents for the photosynthesis process and its low value acts as a limiting factor for the plant growth. Soil analysis results showed that there is an increase in the content (0.36%) of % organic carbon in the soil having degraded hydrogel as compared to the control soil (Table 3).

Phosphorus and potassium are main nutrients, which are required for new plantations and growth of the plants. Potassium and phosphorus in the control soil sample were 12.5 g/m^2 and 59 g/m^2, respectively, but in the Av-cl-poly(AA) degraded soil these components are 13.1 g/m^2 and 59 g/m^2, respectively (Table 3) (Saruchi et al. 2013, 2015).

It was clear from the results that there was only a small change in the pH of the control and test soil sample. The pH was 6.9 in the control sample, and it was 6.7 in the soil with degraded hydrogel, which is in the permissible limit of the soil pH (Table 3).

Conclusion

It was clear from the foregone discussion that a novel aloe vera–acrylic acid-based hydrogel was synthesized. The maximum swelling capacity of the synthesized hydrogel was found to be 756%. Synthesized hydrogel was eco-friendly in nature. It was biodegradable and had no harsh impact on the fertility of the soil; rather it enhanced the soil fertility. Maximum biodegradation was found to be 90%, 94% and 93% in case of soil burial, composting and vermicomposting methods, respectively. It enhanced the water retention and water-holding capacity of clay and sandy loam soil. The water retention periods of soil using synthesized hydrogel prolonged from 11 to 20 days. Synthesized Av-cl-poly(AA) has been found to be effective in sustained release of harmful pesticide dichlorvos. The results showed that maximum release of dichlorvos occurred after 44 h. The maximum release of dichlorvos was found to be 1024.34 ppm. Thus, it can be concluded that synthesized hydrogel is very efficient from agriculture as well as environmental view point.

Acknowledgements

Authors (Saruchi and Vaneet Kumar) are thankful to CT Group of Institutions for carrying out this research work. The authors are grateful to the Researchers Supporting Project number (RSP2023R407), King Saud University, Riyadh, Saudi Arabia, for the financial support

Author contributions

S contributed to conceptualization, methodology and writing—original draft; VK was involved in formal analysis and writing—review and editing; AAG contributed to writing—review and editing; and SP was involved in visualization and writing—review and editing. All authors read and approved the final manuscript.

Funding

The authors are grateful to the Researchers Supporting Project number (RSP2023R407), King Saud University, Riyadh, Saudi Arabia, for the financial support.

Availability of data and materials

The whole data of the present manuscript are available, and it will be provided if asked.

Declarations

Institutional review board statement

Not applicable.

Informed consent

Not applicable.

Competing interests

The authors declare no conflict of interest.

Received: 15 September 2022 Accepted: 25 January 2023
Published online: 17 February 2023

References

Abobatta WF. Hydrogel polymer: a new tool for improving agricultural production. Acad J Polym Sci. 2019;3(2):1–5.
Chen J, Lu S, Zhang Z, Zhao X, Li X, Ning P, Liu M. Environmentally friendly agrochemicals: a review of materials used and their effects on the environment. Sci Total Environ. 2018;613:829–39.
Cheng D, Liu Y, Yang G, Zhang A. Water and agrochemical-integrated hydrogel derived from the polymerization of acrylic acid and urea as a slow-release agrochemical. J Agric Food Chem. 2018;66:5762–9.
Disha J, Begum M, Shawan M, Khatun N, Ahmed S, Islam M, Karim M, Islam M, Hossain M, Hasa M. Preparation and characterization of xanthan gum-based biodegradable polysaccharide hydrogels. J Mater Sci Res. 2016;4:13–8.
Ekebafe LO, Ogbeifun DE, Okieimen FE. Polymer applications in agriculture. Biokemistri. 2011;23:81–9.
Faisal AAH, Al-Wakel SFA, Assi HA, Naji LA, Naushad M. Waterworks sludge-filter sand permeable reactive barrier for removal of toxic lead ions from contaminated groundwater. J Water Process Eng. 2020;33:101112.
Guilherme M, Aouada F, Fajardo A, Martins A, Paulino A, Davi M, Rubira A, Muniz E, Marcos R. Superabsorbent hydrogels based on polysaccharides for application in agriculture as soil conditioner and nutrient carrier: a review. Eur Poly J. 2015;72:365–85.

Han H, Nam D, Seo D, Kim T, Shin B. Preparation and biodegradation of thermosensitive chitosan hydrogel as a function of pH and temperature. Macromol Res. 2004;12:507–11.
Hidangmayum A, Dwivedi P, Katiyar D, Hemantaranjan A. Application of chitosan on plant responses with special reference to abiotic stress. Physiol Mol Biol Plants. 2019;25:313–26.
Hussein A, Khalil B, Abud H. Effect of crosslinking agent ratio and temperature on degree of swelling in polymer hydrogels. Chem pro Engi Res. 2017;52:2224.
Kaith BS, Saruchi, Jindal R, Bhatti MS. Screening and RSM optimization for synthesis of a Gum tragacanth–acrylic acid based device for in situ controlled cetirizine dihydrochloride release. Soft Matter. 2012;8:2286–93.
Kowalski G, Kijowska K, Witczak M, Kuterasinski L, Lukasiewicz M. Synthesis and effect of structure on swelling properties of hydrogels based on high methylated pectin and acrylic polymers. Polymers. 2019;11:114.
Kulkarnia A, Soppimatha K, Aminabhavia T, Dave A, Mehta M. Glutaraldehyde crosslinked sodium alginate beads containing liquid pesticide for soil application. J Control Release. 2000;63:97–105.
Kumar V, De D, Gupta A. Effect of ionic strength on swelling of gelatin hydrogel in marginal solvents. Int J Adv Sci Res. 2015;4:2319–24.
Kwon YR, Kim JS, Kim DH. Effective enhancement of water absorbency of itaconic acid based-superabsorbent polymer via tunable surface-crosslinking. Polymers. 2021;13(16):2782–97.
Mahinroosta M, Jomeh FZ, Allahverdi A, Shakoori Z. Hydrogels as intelligent materials: a brief review of synthesis, properties and applications. Mater Today Chem. 2018;8:42–55.
Michalik R, Wandzik I. A mini-review on chitosan-based hydrogels with potential for sustainable agricultural applications. Polymers. 2020;12:1–16.
Mittal H, Kumar V, et al. Adsorption of methyl violet from aqueous solution using gum xanthan/Fe_3O_4 based nanocomposite hydrogel. Int J Biol Macromol. 2016;89:1–11.
Mittal H, Kumar V, Alhassan SM, Ray SS. Modification of gum ghatti via grafting with acrylamide and analysis of its flocculation, adsorption and biodegradation properties. Int J Biol Macromol. 2018;114:283–94.
Mittal H, Alili AA, Alhassan SM. High efficiency removal of methylene blue dye using carrageenan-poly(acrylamide-co-methacrylic acid)/AQSOA-Z05 zeolite hydrogel composites. Cellulose. 2020;27:8269–85.
Montesanoa F, Parentea A, Santamariab P, Sanninoc A, Serio F. Biodegradable superabsorbent hydrogel increases water retention properties of growing media and plant growth. Agri Agri Sci Procedia. 2015;4:451–8.
Motshabi BR, Ramohoa KE, Modibane KW, Kumar D, Hato MJ, Makhado E. Ultrasonic-assisted synthesis of xanthan gum/ZnO hydrogel nanocomposite for the removal of methylene blue from aqueous solution. Mater Lett. 2022;315:131924.
Nagarjuna G, Babu P, Maruthi Y, Parandhama A, Madhavi C, Subha M, Rao K. Sodium alginate/tragacanth gum blend hydrogel membranes for controlled release of verapamil hydrochloric acid. Indian J Adv Chem Sci. 2016;4:469–77.
Naushad M, Mittal A, Rathore M, Gupta V. Ion-exchange kinetic studies for Cd(II), Co(II), Cu(II), and Pb(II) metal ions over a composite cation exchanger. Desalin Water Treat. 2015;54:2883–90.
Naushad M, et al. Separation of toxic Pb^{2+} metal from aqueous solution using strongly acidic cation-exchange resin: analytical applications for the removal of metal ions from pharmaceutical formulation. Desalin Water Treat. 2015;53:2158–66.
Naushad M, Vasudevan S, Sharma G, Kumar A, Alothman ZA. Adsorption kinetics, isotherms, and thermodynamic studies for Hg^{2+} adsorption from aqueous medium using alizarin red-S-loaded amberlite IRA-400 resin. Desalin Water Treat. 2016;57(39):18551–9.
Naushad M, Alqadami AA, AlOthman ZA, Alsohaimi IH, Algamdi MS, Aldawsari AM. Adsorption kinetics, isotherm and reusability studies for the removal of cationic dye from aqueous medium using arginine modified activated carbon. J Mol Liq. 2019;293:111442.
Neethu TM, Dubey PK, Kaswala AR. Prospects and applications of hydrogel technology in agriculture. Int J Curr Microbiol Appl Sci. 2018;7(5):3155–62.
Ramli RA. Slow release agrochemical hydrogels: a review. Polym Chem. 2019;10:6073–90.
Saruchi, Kumar V. Experimental assessment of the utilization of the novel IPN in different processes in agricultural sector. J Appl Polym Sci. 2019;136(28):1–10.
Saruchi, Kaith BS, et al. Enzyme-based green approach for the synthesis of gum tragacanth and acrylic acid cross-linked hydrogel: its utilization in controlled agrochemical release and enhancement of water-holding capacity of soil. Iran Polym J. 2013;22:561–70.
Saruchi, Kaith BS, et al. Synthesis, characterization and evaluation of Gum tragacanth and acrylic acid hydrogel for sustained calcium chloride release-enhancement of water holding capacity of soil. J Chin Adv Mater Soc. 2014;2:40–52.
Saruchi, Kaith BS, et al. Biodegradation of Gum tragacanth acrylic acid based hydrogel and its impact on soil fertility. Polym Degrad Stab. 2015;115:24–31.
Saruchi, Kaith BS, Kumar V, Jindal R. Biodegradation study of enzymatically catalyzed interpenetrating polymer network: evaluation of agrochemical release and impact on soil fertility. Biotechnol Rep. 2016;9:74–81.
Saruchi, Kumar V, Mittal H, Alhassan SM. Biodegradable hydrogels of tragacanth gum polysaccharide to improve water retention capacity of soil and environment-friendly controlled release of agrochemicals. Int J Biol Macromol. 2019;132:1252–61.
Saruchi, Kaith BS, et al. Sequestration of eosin dye by magnesium (II)-doped zinc oxide nanoparticles: its kinetic, isotherm, and thermodynamic studies. J Chem Eng Data. 2021;66(1):646–57.
Thakur S, Sharma B, Verma A, Chaudhary J, Tamulevicius S, Thakur V. Recent approaches in guar gum hydrogel synthesis for water purification. Int J Polym Anal Charact. 2018;23:621–32.

Publisher's Note